EARTHQUAKE ENGINEERING AND STRUCTURAL DYNAMICS
Earthquake Engng Struct. Dyn. 2000; **29**: 19–36

Effect of stiffness variability on the response of isolated structures

Harry W. Shenton III* and Eric S. Holloway

Department of Civil and Environmental Engineering, University of Delaware, Newark, DE 19716, U.S.A.

SUMMARY

Results are presented of an investigation, the objective of which was to determine the relationship between the stiffness variability of the bearings of an isolation system and the response variability of the structure. The system is modeled as a rigid, rectangular structure that is free to translate and rotate. The isolation system consists of N isolation bearings arranged in a rectangular pattern, each with a stiffness k_i that is an independent, normally distributed, random variable. Response spectrum analysis is used to obtain the analytical solution for the structure response. Approximate closed-form expressions are obtained for the variance of the centreline displacement, rotation, corner displacement and base shear, that are in terms of the variability of the isolator stiffness, aspect ratio of the structure, and the number and layout of isolation bearings. Results show that the standard deviation of the centreline displacement and base shear decrease with increasing number of isolation bearings, and are independent of the aspect ratio and layout of isolators, and in all cases are less than 1/4 the standard deviation of the isolator stiffness. The standard deviation of the corner displacement is a function of all of the system parameters, and is bounded below by the standard deviation of the centreline displacement and above by the standard deviation of a bar aligned perpendicular to the direction of ground motion with m isolation bearings distributed along the length. The approximate expressions are shown to be in good agreement with the results of Monte Carlo simulations. The results should be of use to designers of isolated structures and manufacturers of isolation systems, in assessing the significance of stiffness variability on the response of the isolated structure. Copyright © 2000 John Wiley & Sons, Ltd.

KEY WORDS: analysis; dynamic response; seismic isolation; stiffness; variability

INTRODUCTION

There are numerous seismically isolated structures in the U.S. today and many more around the world. Isolation is now generally considered a viable alternative for seismic hazard mitigation in the design of new structures, and in the rehabilitation of older, deficient buildings and bridges. Furthermore, codes and standards are in place for the design of isolated structures. These include, for buildings the 1997 *Uniform Building Code* (UBC) [1] and the 1997 *NEHRP Provisions* [2],

* Correspondence to: Harry W. Shanton III, Department of Civil and Environmental Engineering, University of Delaware, Newark, DE 19716, U.S.A.

CCC 0098–8847/2000/010019–18$17.50
Copyright © 2000 John Wiley & Sons, Ltd.
Received 5 February 1999
Accepted 28 July 1999

and for bridges the 1991 *Guide Specifications for Seismic Isolation Design* [3]. These codes have and will continue to facilitate the wider use seismic isolation in the future.

Testing is a key component of the design of any isolated structure. Prototype tests of the isolation system are required by UBC and AASHTO to determine the effective stiffness and energy dissipation of the isolation bearings. The results of these tests are used to calculate the design displacements and base shear that are needed for the design of the sub- and superstructures. In almost all cases the isolation system components are also tested before being installed, as the last step in the manufacturing process and as the final test of quality control.

As one might expect, there is inherent variability in the effective stiffness of isolation bearings due to the variability in materials and manufacturing processes. The effective stiffness of a bearing can also vary from one cycle to the next. This variability is explicitly addressed in the 97 UBC, whereby the design displacement (D_D) is calculated using the minimum effective stiffness measured in the prototype tests, and the base shear (V_b) is calculated using the maximum effective stiffness measured in prototype tests. Furthermore, the calculated total design displacement (D_{TM}) at a corner must include an additional contribution due to 'accidental' eccentricity, that is equal to 5 per cent of the maximum dimension of the building in a direction perpendicular to the ground motion. While variability in the properties of a structural component is not unique to isolation systems, the manner in which it is explicitly addressed in the code is unique.

Guidelines for testing isolation systems have been developed [4], and a national consensus standard for testing will soon be available. Included in the test standards are criteria for accepting or rejecting an isolation bearing, based on the difference between the measured effective stiffness and the design or nominal stiffness. Similar criteria are sometimes also adopted in the project specific quality control test program. These criteria, in effect, place a bound on the acceptable stiffness variability of the isolation bearings. To date, the tentative criteria have been based solely on experience and engineering judgement and have typically fallen in the range of 5–10 per cent. The criteria can indirectly control the quality of the isolation component, the cost of the isolation system and the system performance: a criteria that is too stringent will drive the cost of the isolation system up, a criteria that is too liberal may affect the performance of the isolated structure during an earthquake. An acceptable stiffness variability must be established that is consistent with the inherent variability of the other structural components and that takes into consideration the effect it has on the response of the isolated structure. To do this one must examine how the variability of the stiffness of the isolators affects the response variability of the structure.

In a closely related problem, De La Llera and Chopra [5–7] extensively studied the uncertainties that contribute to accidental torsion in buildings. Among the factors considered were rotational motions at the building foundation, uncertainty in the stiffness of structural elements, uncertainty in the location of the structure center of mass, and uncertainty in stiffness and mass distributions of the stories other than the one analyzed. Their model consisted of a rectangular single-storey building that was free to translate and rotate (a two-degree-of-freedom system) [5, 6]. The structure was assumed to have multiple lateral load resisting planes located symmetrically about the centreline of the building, each with a stiffness that varied randomly from the nominal design stiffness. Numerical response spectrum analyses were conducted to study the effects of the stiffness variability [5] and base rotation [6]; results were also compared to those of Monte Carlo simulations [5]. While their studies focused on the response of buildings, many of their findings are applicable to the response of isolated structures. Among their several important conclusions they found: (1) the largest increase in building response comes from uncertainty in the

Copyright © 2000 John Wiley & Sons, Ltd

location of the structure centre of mass and uncertainty in the stiffness of the structural elements, (2) the increase in response due to rotational base excitation is generally small for structures with a fundamental translational period of vibration greater than 1/2 s, (3) the effect of stiffness variability decreases with increasing number of lateral load resisting planes, (4) most sources of uncertainty have a greater effect on nominally symmetric systems than on nominally asymmetric systems, and (5) buildings with a plan dimension perpendicular to the direction of ground motion larger than the other dimension show the greatest increase in response due to accidental torsion.

Hirata *et al.* [8] conducted Monte Carlo simulations of a square rigid structure, supported on 256, uniformly spaced, isolation bearings. The response spectrum analysis showed that the increase in edge displaced due to stiffness variability of the isolators was generally small.

In 1994, De La Llera and Inaudi [9] extended the earlier work of De La Llera and Chopra [5] to that of a seismically isolated structure. In their analysis the isolated structure was modelled as a three-degree-of-freedom system, considering translations in x and y and a rotation, θ. The nominally symmetric structure was assumed to be rectangular in plan and included N isolation bearings located symmetrically about the centreline of the structure. Again, response spectrum analyses were conducted numerically to examine the effects of stiffness variability, and the results were also compared to those of Monte Carlo simulations. The focus of the investigation was on determining how well the code specified requirement for a 5 per cent accidental eccentricity compared to the predicted response, assuming some stiffness variability. Their results showed that the increase in building response due to stiffness uncertainty is smaller than implied by the code specified 5 per cent accidental.

Presented in the following are the results of an investigation, the objective of which was to determine, analytically, the effect of stiffness variability on the response of seismically isolated structures. The isolated structure is modeled as a two-degree-of-freedom system with a rectangular array of isolation bearings. The response of the system is obtained by response spectrum analysis, assuming a predominant first mode response. The key contribution of the work is in the derivation of approximate closed-form expressions for the variance of the system response (centreline displacement, rotation, corner displacement and base shear). Simple expressions are obtained that are in terms of the number and arrangement of isolators, aspect ratio of the structure and the coefficient of variation of the isolator stiffness. Results are presented and are compared to those of numerical simulations. The simple design type equations can be used by designers of isolated structures and isolation manufacturers to assess the impact of stiffness variability on the response of the isolated structure.

ANALYTICAL MODEL

Consider the isolated structure shown in Figure 1. The superstructure is assumed to be rigid and rectangular in plan, with a width b, depth a and mass m_s. Isolation bearings are located symmetrically under the structure and form a uniform rectangular grid with n lines of isolators in the x direction and m lines of isolators in the y direction; the total number of isolators is $m \times n = N$. For simplicity, the outer most isolators are assumed to be located on the perimeter of the structure, spanning a distance of b in the x direction and a in the y direction. The mass moment of inertia of the structure about an axis through the center of gravity can be expressed as $m_s r^2 = m_s b^2(1 + \gamma^2)/12$, where r is the radius of gyration and $\gamma = a/b$ is the aspect ratio of the

Copyright © 2000 John Wiley & Sons, Ltd

structure. Analysis of the motion is restricted to two degrees of freedom; relative displacement in the x direction and rotation θ. The ground acceleration is denoted by $\ddot{x}_g$.

Each isolator is assumed to have a unique stiffness k_i that is equal in both the x and y directions. Furthermore, each stiffness is assumed to be an independent random variable that is normally distributed, with a mean equal to the design or nominal stiffness k_n, and a coefficient of variation equal to the standard deviation divided by the nominal stiffness, $V_{k_i} = V_k = \sigma_k/k_n$.

The governing equations of motion for the two degree of freedom system, with stiffness variability, can be expressed as

$$\begin{bmatrix} m_s & 0 \\ 0 & m_s r^2 \end{bmatrix} \begin{Bmatrix} \ddot{x} \\ \ddot{\theta} \end{Bmatrix} + \begin{bmatrix} \sum_{i=1}^{N} k_i & -\sum_{i=1}^{N} k_i y_i \\ -\sum_{i=1}^{N} k_i y_i & \sum_{i=1}^{N} k_i (x_i^2 + y_i^2) \end{bmatrix} \begin{Bmatrix} x \\ \theta \end{Bmatrix} = -\begin{Bmatrix} m_s \\ 0 \end{Bmatrix} \ddot{x}_g \tag{1}$$

in which x_i and y_i are the co-ordinates of the individual isolation bearings. Equation (1) can be written as

$$\begin{bmatrix} 1 & 0 \\ 0 & 1 \end{bmatrix} \begin{Bmatrix} \ddot{x} \\ r\ddot{\theta} \end{Bmatrix} + \omega_n^2 \begin{bmatrix} \frac{1}{N}\sum_{i=1}^{N} \frac{k_i}{k_n} & -\frac{1}{rN}\sum_{i=1}^{N} \frac{k_i}{k_n} y_i \\ -\frac{1}{rN}\sum_{i=1}^{N} \frac{k_i}{k_n} y_i & -\frac{1}{r^2 N}\sum_{i=1}^{N} \frac{k_i}{k_n} R_i^2 \end{bmatrix} \begin{Bmatrix} x \\ r\theta \end{Bmatrix} = -\begin{Bmatrix} 1 \\ 0 \end{Bmatrix} \ddot{x}_g \tag{2}$$

in which $\omega_n = \sqrt{Nk_n/m_s}$ is the natural frequency of the nominal system in the x direction, assuming no stiffness variability, and $R_i^2 = x_i^2 + y_i^2$. Finally, Equation (2) can be rewritten as

$$\begin{bmatrix} 1 & 0 \\ 0 & 1 \end{bmatrix} \begin{Bmatrix} \ddot{x} \\ r\ddot{\theta} \end{Bmatrix} + \omega_n^2 \begin{bmatrix} K_{11} & K_{12} \\ K_{21} & K_{22} \end{bmatrix} \begin{Bmatrix} x \\ r\theta \end{Bmatrix} = -\begin{Bmatrix} 1 \\ 0 \end{Bmatrix} \ddot{x}_g \tag{3}$$

in which

$$K_{11} = \frac{1}{N}\sum_{i=1}^{N} \frac{k_i}{k_n}; \quad K_{12} = K_{21} = -\frac{1}{Nr}\sum_{i=1}^{N} \frac{k_i}{k_n} y_i; \quad K_{22} = \frac{1}{r^2 N}\sum_{i=1}^{N} \frac{k_i}{k_n} R_i^2 \tag{4}$$

The equations of motion for the nominal system are obtained by substituting $k_i/k_n = 1$ in the previous equations

$$\begin{bmatrix} 1 & 0 \\ 0 & 1 \end{bmatrix} \begin{Bmatrix} \ddot{x}_n \\ r\ddot{\theta}_n \end{Bmatrix} + \omega_n^2 \begin{bmatrix} K_{11_n} & 0 \\ 0 & K_{22_n} \end{bmatrix} \begin{Bmatrix} x_n \\ r\theta_n \end{Bmatrix} = -\begin{Bmatrix} 1 \\ 0 \end{Bmatrix} \ddot{x}_g \tag{5}$$

in which

$$K_{11_n} = 1; \qquad K_{22_n} = \frac{1}{r^2 N}\sum_{i=1}^{N} R_i^2 \tag{6}$$

are the nominal stiffness in the x and θ directions.

Copyright © 2000 John Wiley & Sons, Ltd

ANALYSIS OF THE RESPONSE

The response of the isolated structure is determined by response spectrum analysis. Solving the eigenvalue problem associated with Equation (3) yields, for the frequencies

$$\beta_{1,2} = \frac{K_{11} + K_{22}}{2} \pm \frac{1}{2}[(K_{22} - K_{11})^2 + 4K_{12}K_{21}]^{1/2} \tag{7}$$

in which $\beta_i = \omega_i^2/\omega_n^2$ is the squared ratio of the natural frequency with stiffness variability to the nominal natural frequency in the x direction. The modal matrix can be expressed as

$$[\Phi] = [\phi_1, \phi_2] = \begin{bmatrix} \dfrac{\beta_1 - K_{22}}{\sqrt{(\beta_1 - K_{22})^2 + K_{21}^2}} & \dfrac{K_{21}}{\sqrt{(\beta_2 - K_{22})^2 + K_{21}^2}} \\ \dfrac{K_{12}}{\sqrt{(\beta_1 - K_{22})^2 + K_{21}^2}} & \dfrac{\beta_2 - K_{22}}{\sqrt{(\beta_2 - K_{22})^2 + K_{21}^2}} \end{bmatrix} \tag{8}$$

where the modes have been normalized with respect to the mass (identity) matrix.

Assuming a solution in the modes $\{x\} = [\Phi]\{\eta\}$ yields the uncoupled equations of motion in the generalized co-ordinates η_i,

$$\ddot{\eta}_i + \omega_n^2 \beta_i \eta_i = \{\phi\}_i^T \begin{Bmatrix} -1 \\ 0 \end{Bmatrix} \ddot{x}_g = -\phi_{1i}\ddot{x}_g, \quad i = 1, 2 \tag{9}$$

The maximum response in the generalized co-ordinate η_i is

$$\eta_{i_{max}} = \phi_{1i} S_{D_i} \tag{10}$$

in which S_{D_i} is the spectral displacement corresponding to the period $T_i = 2\pi/\omega_n\sqrt{\beta_i}$ and damping ratio ζ_i.

The fundamental period of most isolated structures is in the range of 1.5 to 3.5 s. In this regime the elastic design spectral acceleration can be expressed as $S_A = C_{VD}\, g/T$ [1], in which T is the period of vibration and g is the acceleration due to gravity. Therefore, the elastic spectral displacement for mode i is

$$S_{D_i} = \frac{S_{A_i}}{B_D \omega_i^2} = \frac{C_{VD}\, g}{B_D T_i} \frac{T_i^2}{4\pi^2} = \frac{C_{VD}\, g}{2\pi B_D \omega_n \sqrt{\beta_i}} \tag{11}$$

in which B_D is the code adjustment factor for the increased damping of the isolation system.

Assuming a first mode response, which is generally accurate for most isolated structures, the maximum response of the structure is

$$\{x\}_{max} \approx \{\phi\}_1 \eta_{1_{max}} = \begin{Bmatrix} \phi_{11} \\ \phi_{21} \end{Bmatrix} \times \frac{C_{VD}\, g}{2\pi B_D \omega_n \sqrt{\beta_i}} \times \phi_{11} \tag{12}$$

therefore, the maximum center displacement of the structure and the maximum rotation are

$$x_{max} = \frac{C_{VD} g \phi_{11}^2}{2\pi B_D \omega_n \sqrt{\beta_1}}, \qquad r\theta_{max} = \frac{C_{VD} g \phi_{11} \phi_{21}}{2\pi B_D \omega_n \sqrt{\beta_1}} \tag{13}$$

Copyright © 2000 John Wiley & Sons, Ltd

The maximum corner displacement can be expressed as

$$x_{c_{\max}} = x_{\max} \pm \frac{a}{2r} r\theta_{\max} = \frac{C_{\mathrm{VD}} g \phi_{11}^2}{2\pi B_{\mathrm{D}} \omega_{\mathrm{n}} \sqrt{\beta_1}} \pm \frac{a}{2r} \frac{C_{\mathrm{VD}} g \phi_{11} \phi_{21}}{2\pi B_{\mathrm{D}} \omega_{\mathrm{n}} \sqrt{\beta_1}} \tag{14}$$

The response of the nominal system (no variability) is obtained by letting $k_i / k_{\mathrm{n}} = 1$ in Equations (7)–(14): this yields $\beta_1 = 1$ and $\beta_2 = K_{22_{\mathrm{n}}}$, and the modal matrix reduces to the identity matrix. Referring to Equation (13), the maximum nominal centreline displacement is $x_{\mathrm{n}_{\max}} = C_{\mathrm{VD}} g / 2\pi B_{\mathrm{D}} \omega_{\mathrm{n}}$ and as would be expected, the nominal rotation of the structure is zero. Dividing the expressions in Equation (13) by $x_{\mathrm{n}_{\max}}$ yields

$$\bar{x} = \frac{x_{\max}}{x_{\mathrm{n}_{\max}}} = \frac{\phi_{11}^2}{\sqrt{\beta_1}} = g_x(k_i), \qquad \bar{\theta} = \frac{r\theta_{\max}}{x_{\mathrm{n}_{\max}}} = \frac{\phi_{11}\phi_{21}}{\sqrt{\beta_1}} = g_\theta(k_i) \tag{15}$$

Finally, after introducing the expression for r and simplifying, the normalized corner displacement can be expressed as

$$\bar{x}_c = \frac{x_{c_{\max}}}{x_{\mathrm{n}_{\max}}} = \frac{\phi_{11}^2}{\sqrt{\beta_1}} \pm \frac{\sqrt{3}\gamma}{\sqrt{1+\gamma^2}} \frac{\phi_{11}\phi_{21}}{\sqrt{\beta_1}} = g_{\mathrm{c}}(k_i) \tag{16}$$

The base shear due to deformation in the x direction is equal to $V_{\mathrm{b}} = (\sum k_i) x$. Substituting the expression for x from Equation (13) and simplifying, this can be expressed as

$$\frac{V_{\mathrm{b}}}{m_{\mathrm{s}}} = \frac{\omega_{\mathrm{n}}^2}{N} \left(\sum \frac{k_i}{k_{\mathrm{n}}} \right) \frac{C_{\mathrm{VD}} g \phi_{11}^2}{2\pi B_{\mathrm{D}} \omega_{\mathrm{n}} \sqrt{\beta_1}} \tag{17}$$

and the nominal base shear is

$$\left(\frac{V_{\mathrm{b}}}{m_{\mathrm{s}}} \right)_{\mathrm{n}} = \frac{\omega_{\mathrm{n}} C_{\mathrm{VD}} g}{2\pi B_{\mathrm{D}}} \tag{18}$$

Dividing Equation (17) by Equation (18) yields the normalized base shear

$$\bar{V}_{\mathrm{b}} = \frac{1}{N} \left(\sum \frac{k_i}{k_{\mathrm{n}}} \right) \frac{\phi_{11}^2}{\sqrt{\beta_1}} = K_{11} \frac{\phi_{11}^2}{\sqrt{\beta_1}} = g_V(k_i) \tag{19}$$

Equations (15) and (16) are approximate closed-form expressions for the maximum centre displacement, rotation and corner displacement of the isolated structure, normalized by the centre displacement assuming no stiffness variability. Likewise, Equation (19) is an approximate expression for the base shear, normalized by the nominal base shear, assuming no variability. They are each functions of the aspect ratio of the structure (γ), the number and layout of isolators (n, m), and the stiffness of the individual isolators (k_i).

ANALYSIS OF THE MEAN AND VARIANCE

With functional relationships between the random stiffness of the isolators and the displacement, rotation and base shear of the structure (Equations (15), (16) and (19)), the mean and variance of the response can be estimated from the mean and variance of the stiffness [10].

Copyright © 2000 John Wiley & Sons, Ltd

Consider first the displacement at the centre of the structure ($\bar{x}$). Expanding the equation for $\bar{x}$ in Equation (15) in a Taylor series about the mean values $k_i = k_n$, yields

$$g_x(k_1, k_2, \ldots, k_N) = g_x(k_1 = k_n, k_2 = k_n, \ldots, k_N = k_n) + \sum_{i=1}^{N} (k_i - k_n) \frac{\partial g_x}{\partial k_i} + \frac{1}{2} \sum_{i=1}^{N} \sum_{j=1}^{N} (k_i - k_n)(k_j - k_n) \frac{\partial^2 g_x}{\partial k_i \partial k_j} + \cdots \tag{20}$$

in which all of the partial derivatives are evaluated at the mean value k_n. Retaining only the linear terms, the first-order approximate mean is

$$E(\bar{x}) \approx g_x(k_1 = k_n, k_2 = k_n, \ldots, k_N = k_n) \tag{21}$$

The first-order variance of $\bar{x}$ is

$$\mathrm{Var}(\bar{x}) \approx \sum_{i=1}^{N} \left(\frac{\partial g_x}{\partial k_i} \right)^2 \mathrm{Var}(k_i) + \sum_{i \neq j}^{N} \sum^{N} \frac{\partial g_x}{\partial k_i} \frac{\partial g_x}{\partial k_j} \mathrm{Cov}(k_i, k_j) \tag{22}$$

in which $\mathrm{Var}(k_i)$ is the variance of the stiffness k_i and $\mathrm{cov}(k_i, k_j)$ is the covariance between k_i and k_j. Assuming the individual stiffness are uncorrelated (a conservative assumption), the variance becomes

$$\mathrm{Var}(\bar{x}) \approx \sum_{i=1}^{N} \left(\frac{\partial g_x}{\partial k_i} \right)^2 \mathrm{Var}(k_i) \tag{23}$$

The mean and variance of $\bar{x}_c, \bar{\theta}$ nd $\bar{V}_b$ are obtained in a similar manner by using the partial derivative of the approximate function $g_c(k_i)$, $g_\theta(k_i)$ and $g_V(k_i)$, respectively, in Equations (21) and (23).

Analysis of the mean

Referring to Equation (21), to first order, the mean values are obtained by evaluating the equations for $\bar{x}$, $\bar{\theta}$, $\bar{x}_c$ and $\bar{V}_b$ at the nominal stiffness k_n. Letting $k_i = k_n$ in Equations (7) and (8), yields for the fundamental frequency and mode shape: $\beta_1 = 1$, $\phi_{11} = 1$ and $\phi_{21} = 0$. Substituting these results into Equations (15), (16) and (19) yields

$$E(\bar{x}) = 1, \qquad E(\bar{\theta}) = 0, \qquad E(\bar{x}_c) = 1, \qquad E(\bar{V}_b) = 1 \tag{24}$$

Analysis of the variance

To calculate the variances the partial derivatives of the four functions g_x, g_θ, g_c and g_V with respect to k_i, evaluated at k_n are needed. Details of these derivations are presented in the Appendix, the results are presented below:

$$\left. \frac{\partial g_x}{\partial k_i} \right|_{k_n} = -\frac{1}{2Nk_n} \tag{25}$$

$$\left. \frac{\partial g_\theta}{\partial k_i} \right|_{k_n} = \frac{-y_i}{Nrk_n(1 - K_{22_n})} = \frac{-y_i r}{k_n(Nr^2 - \sum R_i^2)} \tag{26}$$

Copyright © 2000 John Wiley & Sons, Ltd

$$\left.\frac{\partial g_c}{\partial k_i}\right|_{k_n} = -\frac{1}{2Nk_n} \pm \frac{\sqrt{3}\gamma}{\sqrt{1+\gamma^2}} \frac{y_i}{Nrk_n(1-K_{22_n})} \tag{27}$$

$$\left.\frac{\partial g_v}{\partial k_i}\right|_{k_n} = \frac{1}{2Nk_n} \tag{28}$$

Substituting Equation (25) into Equation (23), the variance of $\bar{x}$ is

$$\mathrm{Var}(\bar{x}) = \sum_{i=1}^{N} \frac{1}{4N^2k_n^2} \mathrm{Var}(k_i) \tag{29}$$

Letting $\mathrm{Var}(k_i) = (V_k k_n)^2$, this reduces to

$$\mathrm{Var}(\bar{x}) = \sum_{i=1}^{N} \frac{1}{4N^2k_n^2} V_k^2 k_n^2 = \frac{V_k^2}{4N} \tag{30}$$

Therefore, the standard deviation of the displacement at the centre of the structure is

$$\sigma_{\bar{x}} = V_k/2\sqrt{N} \tag{31}$$

Substituting Equation (26) into the equation for the variance of $\bar{\theta}$ yields

$$\mathrm{Var}(\bar{\theta}) \approx \sum_{i=1}^{N} \left(\frac{\partial g_\theta}{\partial k_i}\right)^2 \mathrm{Var}(k_i) = \sum_{i=1}^{N} \left\{\frac{-y_i}{Nrk_n(1-K_{22_n})}\right\}^2 \mathrm{Var}(k_i) \tag{32}$$

Again, letting $\mathrm{Var}(k_i) = (V_k k_n)^2$ yields

$$\mathrm{Var}(\bar{\theta}) \approx \sum_{i=1}^{N} \left\{\frac{-y_i}{Nrk_n(1-K_{22_n})}\right\}^2 V_k^2 k_n^2 = \frac{V_k^2}{N^2r^2\left(1-\dfrac{\sum R_i^2}{Nr^2}\right)^2} \sum_{i=1}^{N} y_i^2 \tag{33}$$

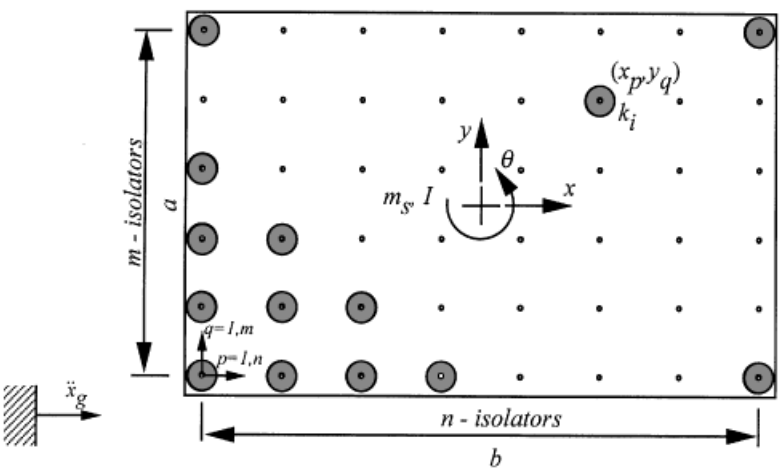

Figure 1. Definition diagram: plan view of isolated structure.

Copyright © 2000 John Wiley & Sons, Ltd

Referring to Figure 1, the x, y co-ordinates of isolator p, q can be expressed as

$$x_p = \frac{b}{2}\left(\frac{2(p-1)}{n-1} - 1\right), \quad p = 1, \ldots, n \tag{34}$$

$$y_q = \frac{a}{2}\left(\frac{2(q-1)}{m-1} - 1\right), \quad q = 1, \ldots, m \tag{35}$$

Using these relations, it can be shown that the summation in y_i^2 and x_i^2 in Equation (33) can be expressed as

$$\sum_{i=1}^{N} x_i^2 = m \sum_{p=1}^{n} \left\{\frac{b}{2}\left(\frac{2(p-1)}{n-1} - 1\right)\right\}^2 = \frac{b^2 N}{12}\frac{n+1}{n-1} = \frac{b^2 N \bar{n}}{12} \tag{36}$$

$$\sum_{i=1}^{N} y_i^2 = n \sum_{q=1}^{m} \left\{\frac{a}{2}\left(\frac{2(q-1)}{m-1} - 1\right)\right\}^2 = \frac{a^2 N}{12}\frac{m+1}{m-1} = \frac{a^2 N \bar{m}}{12} \tag{37}$$

in which

$$\bar{m} = \frac{m+1}{m-1}; \qquad \bar{n} = \frac{n+1}{n-1} \tag{38}$$

therefore

$$\sum_{i=1}^{N} R_i^2 = \sum_{i=1}^{N} x_i^2 + \sum_{i=1}^{N} y_i^2 = \frac{b^2 N}{12}\{\bar{n} + \bar{m}\gamma^2\} \tag{39}$$

The term involving R_i in the denominator of Equation (33) can be expressed as

$$\frac{\sum R_i^2}{Nr^2} = \frac{\bar{n} + \bar{m}\gamma^2}{1 + \gamma^2} \tag{40}$$

Finally, substituting these results into Equation (33) and simplifying yields

$$\mathrm{Var}(\bar{\theta}) = \frac{V_k^2}{N}\frac{(1+\gamma^2)\gamma^2\bar{m}}{\{(1-\bar{n}) + (1-\bar{m})\gamma^2\}^2} \tag{41}$$

Therefore, the standard deviation in $\bar{\theta}$ is given by

$$\sigma_{\bar{\theta}} = \frac{V_k}{2\sqrt{N}}\left[\frac{4\gamma^2(1+\gamma^2)}{[(1-\bar{n}) + (1-\bar{m})\gamma^2]^2}\right]^{1/2} \tag{42}$$

Proceeding in a similar manner, the standard deviation in $\bar{x}_c$ is

$$\sigma_{\bar{x}_c} = \frac{V_k}{2\sqrt{N}}\left[1 + \frac{12\gamma^4\bar{m}}{[(1-\bar{n}) + (1-\bar{m})\gamma^2]^2}\right]^{1/2} \tag{43}$$

where it can be shown that the " $\pm$ " in Equation (27) is inconsequential to the final result. The standard deviation in the normalized base shear, $\bar{V}_b$, is

$$\sigma_{\bar{V}_b} = V_b/2\sqrt{N} \tag{44}$$

Copyright © 2000 John Wiley & Sons, Ltd

Equations (31), (42), (43) and (44) are approximate closed-form expressions for the standard deviation of the centreline displacement, rotation, corner displacement and base shear of the isolated structure, expressed in terms of the aspect ratio, number and layout of the isolators and the coefficient of variation of the isolator stiffness. They are simple, explicit relations between the variance of the isolator stiffness and the variance of the structural response.

MONTE CARLO SIMULATIONS

Monte Carlo simulations were conducted for the purpose of comparing the approximate closed-form results with the 'exact' numerical results. The maximum centreline displacement, corner displacement, rotation and base shear of the system were calculated by response spectrum analysis. As with the analytical formulation, the numerical results were obtained for a single mode response using the elastic design spectrum of the 1997 Uniform Building Code. Results were normalized by the nominal response assuming no variability.

Simulations were conducted for a number of different system configurations. This included aspect ratios of $\gamma = a/b = 1/4, 1, 4$ and 10, and the number of isolators (N) ranging from 4 to 2500, arranged in different n by m patterns. For each configuration a total of 2000 simulations were carried out. The stiffness of each isolator was randomly selected assuming a normal distribution with a specified coefficient of variation (i.e. stiffness variability). Upon completion of the analyses, the mean and standard deviation of the various response quantities were calculated from the sample of 2000 events.

RESULTS AND DISCUSSION

Presented in Figure 2 is the standard deviation of the displacement $\bar{x}$ versus the total number of isolators, N. Also shown in the figure, as indicated by the discrete data points are the results of the Monte Carlo simulations. Numerical results are shown for aspect ratios of 1/4, 1 and 4, and all possible m, n permutations of 2, 5, 10 and 15 ($4 \leqslant N \leqslant 225$).

For these results the stiffness coefficient of variation (V_k) was determined based on an assumed stiffness *variability* of 5, 10 or 20 per cent: stiffness *variability* is defined here as three times the standard deviation of the stiffness and is intended to represent a typical value that might be specified in a test standard or quality control program. Assuming a normal distribution, and that the stiffness of each isolator must be within $\pm 3\sigma$ of the mean stiffness, results are presented for $V_k = 5/3$, 10/3 and 20/3 per cent.

Equation (31) and Figure 2 show that the standard deviation of the centreline displacement decreases rapidly with increasing number of isolators: this is consistent with the results of De La Lera and Chopra [5]. The theoretical prediction is also found to be in good agreement with the results of the simulations, particularly for lower values of V_k. In all cases the approximate closed-form expression is within 5 per cent of the numerical results, for $V_k = 5/3$ and 10/3 per cent. The accuracy of Equation (31) decreases with increasing V_k and also with increasing γ, as shown in Figure 2(c). In this case the approximate results differ by as much as 20 per cent relative to the numerical.

The numerical simulations also confirm that the variance in $\bar{x}$ in general independent of the aspect ratio (γ), and independent of the particular values of m and n, as evident by the theoretical

Copyright © 2000 John Wiley & Sons, Ltd

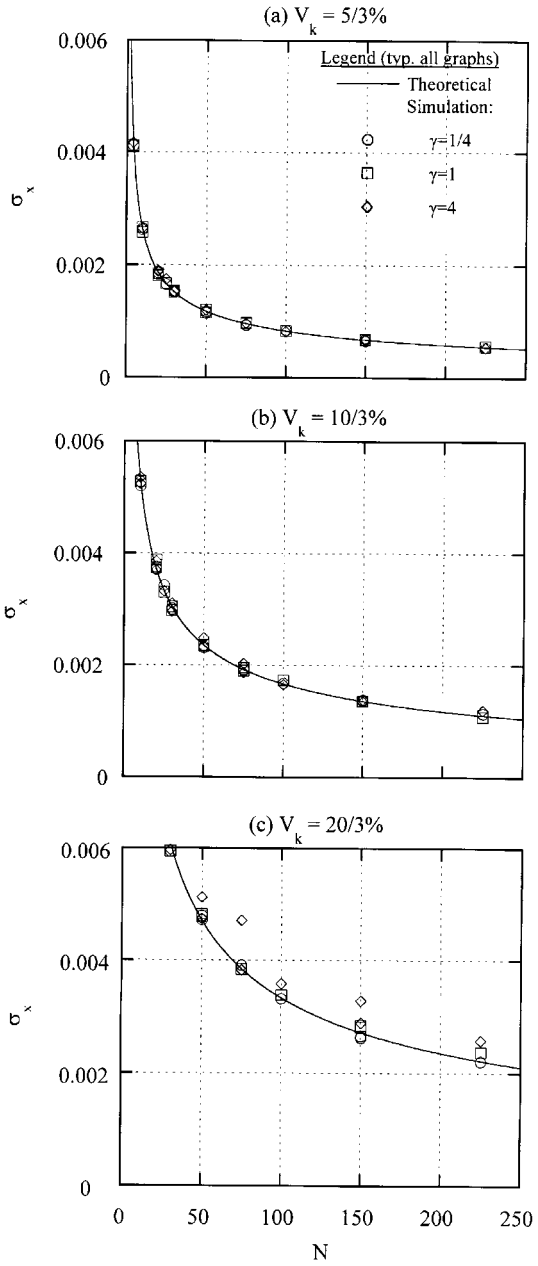

Figure 2. Standard deviation of centreline displacement ($\bar{x}$) versus number of isolation bearings: (a) $V_k = 5/3$ per cent, (b) $V_k = 10/3$ per cent, (c) $V_k = 20/3$ per cent.

Copyright © 2000 John Wiley & Sons, Ltd

expression (31). This would be expected since the structure and isolator layout are both symmetric about the x- and y-axis. This is certainly true for lower V_k; for $V_k = 20$ per cent the numerical results suggest that the variance in $\bar{x}$ increases slightly with increasing γ.

Similar results are presented in Figure 3 for the base shear, $\bar{V}_b$. The approximate theoretical expressions for the standard deviation of the centreline displacement and the base shear are identical, and this is confirmed by the numerical results. Comparing Figures 2 and 3, the agreement and trends noted previously for the centreline displacement are identical for the base shear.

It is worth noting that the standard deviation of the centreline displacement and the base shear are both bounded by 1/2 the coefficient of variation (i.e. standard deviation, since $E(\bar{x}) = 1$)) of the isolator stiffness. Furthermore, since $N \geqslant 4$ for any practical isolated structure, the standard deviation of $\bar{x}$ and V_b will always be less than 1/4 the coefficient of variation of the isolator stiffness. For a moderate sized isolation system with 25 isolators, this reduces to just 1/10 that of the isolator stiffness. Expressed another way, assuming an allowable stiffness variability of 5 per cent, the results show that in the worst case the centreline displacement and base shear of the structure will be within ± 1.25 per cent of the design, for a system with 4 isolators, and within ± 0.5 per cent for a system with 25 isolators. These results indicate that, at least in terms of centreline displacement and base shear, an unduly tight restriction on the allowable variability of isolator stiffness may not be justified, since the structural response variability due to other influences could far exceed the effects of the stiffness variability of the isolation system.

Presented in Figure 4 are the results for the standard deviation of the corner displacement $\bar{x}_c$, as a function of the aspect of ratio γ. Note, referring to Equation (43), that the standard deviation of the corner displacement is also proportional to V_k; therefore, in this case the results in Figure 4 have been normalized by V_k. Results are shown for three values of n (2, 10 and 50) and four values of m (2, 5, 10 and 50). Once again, also shown in the figures are the results of the Monte Carlo simulations.

The standard deviation of the corner displacement is found to be a function of all of the system parameters, including γ, V_k and N. Furthermore, it is not only varies with N, but with the particular m, n layout of the isolators. In all cases, the standard deviation of $\bar{x}_c$ decreases with increasing n. This can be explained as follows: with m held constant, as n increases the total stiffness of any given x line of isolators tends towards nk_n. This tends to reduce the accidental eccentricity due to stiffness variability and therefore, also the corner displacement. The standard deviation of $\bar{x}_c$ decreases with increasing m, for small γ, but increases with increasing m for large γ. For a wide range of n and m combinations, the standard deviation of the corner displacement is less than the stiffness coefficient of variation. As before, the approximate closed-form expression for the standard deviation of $\bar{x}_c$ is in good agreement with the numerical results. The accuracy of Equation (44) is approximately the same for all n; the accuracy decreases slightly with increasing γ and increasing m.

It is interesting to note that σ_{x_c}/V_k increases rapidly with γ, and then asymptotes to a constant value for large γ. Equation (43), in fact, reduces to Equation (31) when $\gamma = 0$, as it should since the variance of the corner displacement should reduce to that of the centre as the depth of the structure tends to zero ($a \to 0$). It can be shown that there are no local maxima to σ_{x_c} between $\gamma = 0$ and $\gamma \to \infty$; therefore, the standard deviation of the corner displacement is bounded above by the asymptote value of Equation (43) for large γ. Taking the limit of σ_{x_c}/V_k as $\gamma \to \infty$ yields

$$\lim_{\gamma \to \infty} \left\{ \frac{\sigma_{x_c}}{V_k} \right\} = \frac{V_k}{2\sqrt{N}} \left[1 + \frac{12\bar{m}}{(1-\bar{m})^2} \right]^{1/2} \tag{45}$$

Copyright © 2000 John Wiley & Sons, Ltd

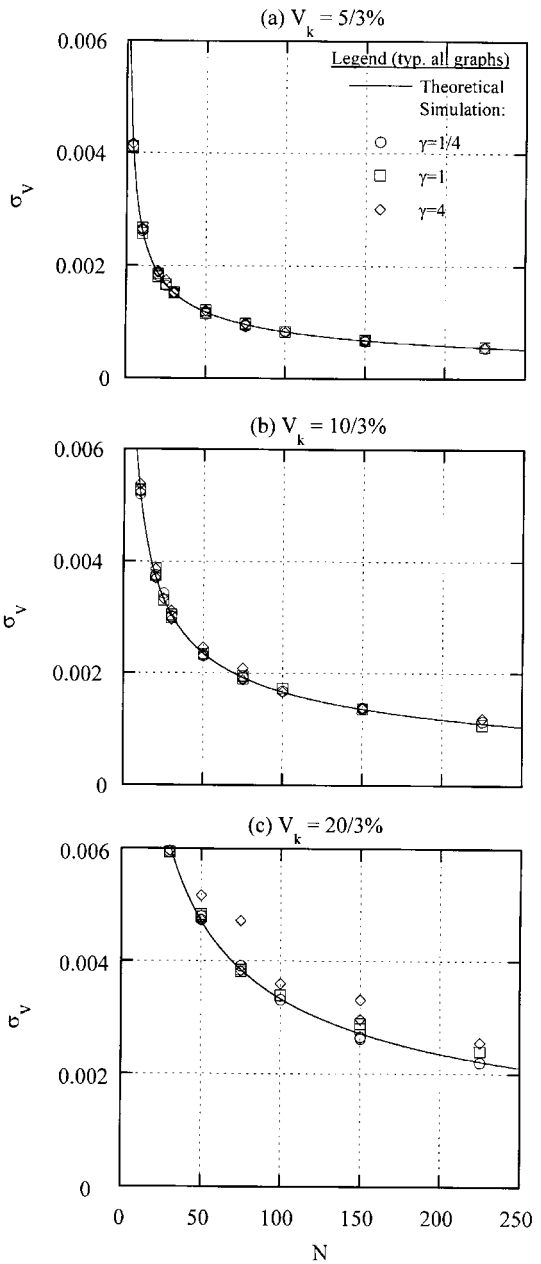

Figure 3. Standard deviation of base shear ($\bar{V}_b$) versus number of isolation bearings: (a) $V_k = 5/3$ per cent, (b) $V_k = 10/3$ per cent, (c) $V_k = 20/3$ per cent.

Copyright © 2000 John Wiley & Sons, Ltd

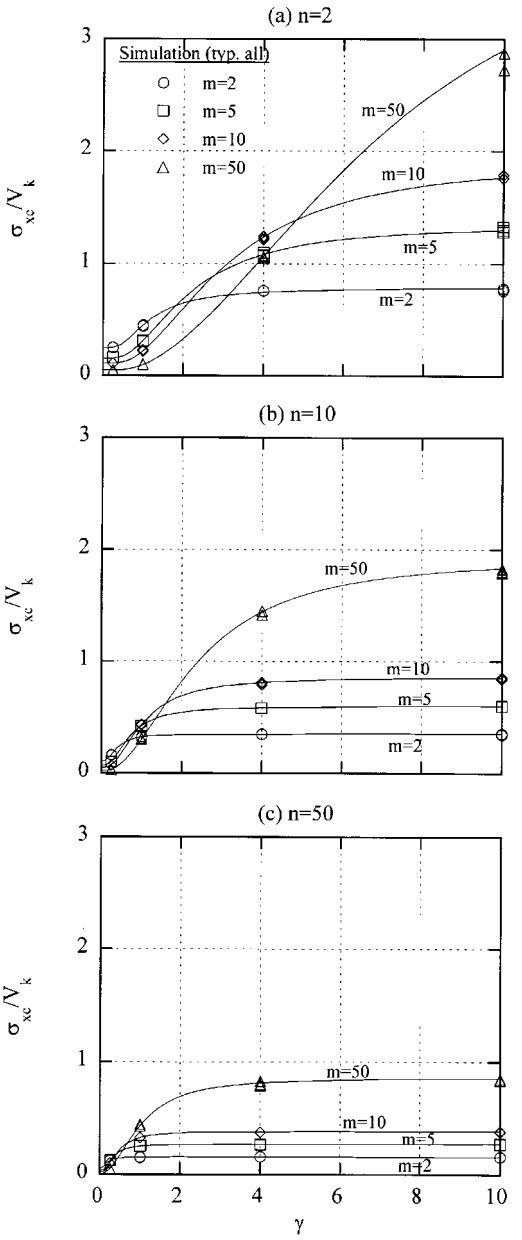

Figure 4. Standard deviation of corner displacement normalized by V_k versus γ: (a) $n = 2$, (b) $n = 10$, (c) $n = 50$.

Copyright © 2000 John Wiley & Sons, Ltd

This is equivalent to the standard deviation of the tip displacement of a bar of length a, that is parallel to the y-axis and is supported on m isolation bearings along its length. Equation (45) can also be obtained by carrying out the analysis of the variance for a bar, by letting $N = m$ and $r^2 = a^2/12$ in the derivation of σ_{x_c}. Equation (45) is convenient because it provides an upper bound to σ_{x_c} that is only a function of the coefficient of variation of the isolator stiffness (V_k) and the layout of the isolators (m, n).

Finally, it is worth comparing the maximum possible corner displacement with the UBC code requirement for accidental eccentricity [1]. The code equation for the corner displacement is, in the notation used herein

$$x_c = x\left[1 + y\frac{12e}{b^2 + a^2}\right] \tag{46}$$

in which y is the distance to the isolation bearing in question, and e is the actual plus accidental eccentricity, the latter of which is equal to 5 per cent of the maximum structure dimension in a direction perpendicular to the direction of force under consideration. Substituting $y = a/2$ and $e = 0.05a$ in Equation (46) and simplifying yields,

$$\frac{x_c}{x} = 1 + \frac{0.3\gamma^2}{1 + \gamma^2} \tag{47}$$

Equation (47) is plotted in Figure 5 versus γ. Also shown in the figure is the mean plus three standard deviation corner displacement as given by Equation (43). Results are presented for $n = 2$ and $m = 50$. Note that for stiffness coefficients of variation of 5/3 per cent and 10/3 per cent, the

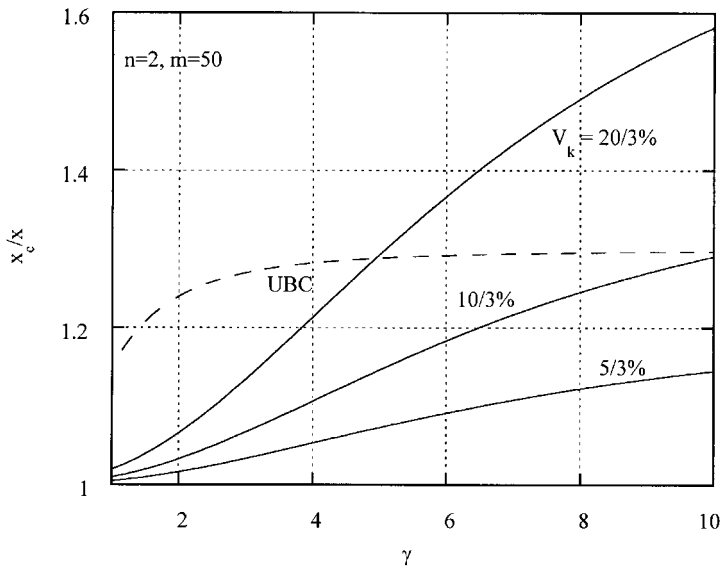

Figure 5. Comparison of the UBC equation for maximum corner displacement and the mean-plus-three-sigma corner displacement, for three values of V_k.

Copyright © 2000 John Wiley & Sons, Ltd

code equation is conservative for γ less than 10. The code equation is also conservative for γ less than approximately 5, for a stiffness coefficient of variation of 20/3 per cent, but underestimates the maximum corner displacement for γ greater than five. These results are for a layout ($n = 2$, $m = 50$) that accentuates the torsional response; in any practical structure, where n is greater than 2, the code equation will in general be conservative, even for stiffness variables as high as 20 per cent.

CONCLUSIONS

A study has been conducted to determine the relationship between the stiffness variability in a seismically isolated structure, and the structural response variability. Based on the results of this investigation, the following conclusions can be stated:

1. Approximate closed-form expressions have been obtained for the standard deviation of the centreline displacement, base shear, rotation and corner displacement of an isolated structure, that are in terms of the coefficient of variation of the isolator stiffness (V_k), aspect ratio of the structures (γ), and the number (N) and layout of the isolators (n, m). The equations provide simple, explicit relations between the isolator variability and the structural response variability.
2. The standard deviation of the centreline displacement and the base shear of the structure (a) decrease with increasing number of isolators, (b) are generally independent of the aspect ratio and layout of the isolators and (c) are less than 25 per cent of the coefficient of variation of the isolator stiffness, for all practical isolated structures, where $N \geqslant 4$.
3. The standard deviation of the corner displacement is influenced by all of the system parameters. The standard deviation of the corner displacement (a) decreases with n, (b) increases or decreases with m, depending on the aspect ratio, and (c) is bounded below by the standard deviation of the corner displacement and above by the standard deviation of an isolated structure that is modeled as a bar perpendicular to the direction of ground motion, with m isolators distributors along its length. The standard deviation of the corner displacement is less than that of the isolators for a wide range of aspect ratios and isolators layouts.
4. The predicted mean plus three sigma corner displacement is less than that required by the UBC for accidental eccentricity, for a broad range of practical isolator layouts, variabilities and structure aspect ratios.
5. The approximate closed-form expressions have been shown to be in good agreement with the results of Monte Carlo simulations. The accuracy of the theoretical expressions decreases slightly with increasing m and increasing γ.
6. Results suggest that an unduely tight criteria on the allowable stiffness variability of seismic isolation bearings is not justified, given that the variability of the centreline displacement and base shear will in all cases be lower than the stiffness variability of the bearings, and for a broad range of system parameters so will the variability of the corner displacement.

It is hoped that the equations derived herein will of use to designers of isolated structures and to manufacturers of isolation bearings, in assessing the significance of stiffness variability on the response variability of isolated structures.

Copyright © 2000 John Wiley & Sons, Ltd

APPENDIX A

The partial derivatives of $g_x(k_i)$, $g_\theta(k_i)$, $g_c(k_i)$ and $g_V(k_i)$, needed in evaluating the variances of $\bar{x}$, $\bar{x}_c$, $\bar{\theta}$ and $\bar{V}_b$ as defined in Equation (23) are given below.

$$\left.\frac{\partial g_x}{\partial k_i}\right|_{k_n} = \left.\frac{\partial}{\partial k_i}\left(\frac{\phi_{11}^2}{\sqrt{\beta_1}}\right)\right|_{k_n} = \left.\left\{\frac{2\phi_{11}}{\sqrt{\beta_1}}\frac{\partial\phi_{11}}{\partial k_i} - \frac{1}{2}\frac{\phi_{11}^2}{\beta_1^{3/2}}\frac{\partial\beta_1}{\partial k_i}\right\}\right|_{k_n} \tag{A1}$$

$$\left.\frac{\partial g_\theta}{\partial k_i}\right|_{k_n} = \left.\frac{\partial}{\partial k_i}\left(\frac{\phi_{11}\phi_{21}}{\sqrt{\beta_1}}\right)\right|_{k_n} = \left.\left\{\frac{\phi_{11}}{\partial k_i}\frac{\phi_{21}}{\sqrt{\beta_1}} + \frac{\phi_{11}}{\sqrt{\beta_1}}\frac{\partial\phi_{21}}{\partial k_i} - \frac{1}{2}\frac{\phi_{11}\phi_{21}}{\beta_1^{3/2}}\frac{\partial\beta_1}{\partial k_i}\right\}\right|_{k_n} \tag{A2}$$

$$\begin{aligned}\left.\frac{\partial g_c}{\partial k_i}\right|_{k_n} &= \left.\frac{\partial}{\partial k_i}\left(\frac{\phi_{11}^2}{\sqrt{\beta_1}} \pm \frac{\sqrt{3}\gamma}{(\gamma^2+1)^{1/2}}\frac{\phi_{11}\phi_{21}}{\sqrt{\beta_1}}\right)\right|_{k_n} \\ &= \left.\left\{\frac{\partial}{\partial k_i}\left(\frac{\phi_{11}^2}{\sqrt{\beta_1}}\right) + \frac{\sqrt{3}\gamma}{(\gamma^2+1)^{1/2}}\frac{\partial}{\partial k_i}\left(\frac{\phi_{11}\phi_{21}}{\sqrt{\beta_1}}\right)\right\}\right|_{k_n}\end{aligned} \tag{A3}$$

$$\left.\frac{\partial g_V}{\partial k_i}\right|_{k_n} = \left.\frac{\partial}{\partial k_i}\left(\frac{K_{11}\phi_{11}^2}{\sqrt{\beta_1}}\right)\right|_{k_n} = \left.\left\{\frac{\phi_{11}^2}{\sqrt{\beta_1}}\frac{\partial K_{11}}{\partial k_i} + \frac{2K_{11}\phi_{11}}{\sqrt{\beta_1}}\frac{\partial\phi_{11}}{\partial k_i} - \frac{1}{2}\frac{K_{11}\phi_{11}^2}{\beta_1^{3/2}}\frac{\partial\beta_1}{\partial k_i}\right\}\right|_{k_n} \tag{A4}$$

Evaluating the various partial derivatives in these expressions yields

$$\begin{aligned}\frac{\partial\phi_{11}}{\partial k_i} &= \left\{\frac{\partial\beta_1}{\partial k_i} - \frac{\partial K_{22}}{\partial k_i}\right\}\{(\beta_1 - K_{22})^2 + K_{21}^2\}^{-1/2} - \frac{1}{2}(\beta_1 - K_{22}) \\ &\quad \times\{(\beta_1 - K_{22})^2 + K_{21}^2\}^{-3/2}\left\{2(\beta_1 - K_{22})\left(\frac{\partial\beta_1}{\partial k_i} - \frac{\partial K_{22}}{\partial k_i}\right) + 2K_{21}\frac{\partial K_{21}}{\partial k_i}\right\}\end{aligned} \tag{A5}$$

$$\begin{aligned}\frac{\partial\phi_{21}}{\partial k_i} &= \frac{\partial K_{21}}{\partial k_i}\{(\beta_1 - K_{22})^2 + K_{21}^2\}^{-1/2} - \frac{1}{2}K_{21}\{(\beta_1 - K_{22})^2 + K_{21}^2\}^{-3/2} \\ &\quad \times\left\{2(\beta_1 - K_{22})\left(\frac{\partial\beta_1}{\partial k_i} - \frac{\partial K_{22}}{\partial k_i}\right) + 2K_{21}\frac{\partial K_{21}}{\partial k_i}\right\}\end{aligned} \tag{A6}$$

$$\begin{aligned}\frac{\partial\beta_i}{\partial k_i} &= \frac{1}{2}\left\{\frac{\partial K_{11}}{\partial k_i} + \frac{\partial K_{22}}{\partial k_i}\right\} \pm \frac{1}{2}\left\{\frac{1}{4}(K_{11} - K_{22})^2 + K_{12}K_{21}\right\}^{-1/2} \\ &\quad \times\left\{\frac{1}{2}(K_{11} - K_{22})\left(\frac{\partial K_{11}}{\partial k_i} - \frac{\partial K_{22}}{\partial k_i}\right) + 2K_{21}\frac{\partial K_{21}}{\partial k_i}\right\}\end{aligned} \tag{A7}$$

Recalling that $K_{12} = K_{21} = 0$ when evaluated at the nominal stiffness $k_i = k_n$, these reduce to

$$\partial\phi_{11}/\partial k_i = 0 \tag{A8}$$

$$\frac{\partial\phi_{21}}{\partial k_i} = \left.\frac{\partial K_{21}}{\partial k_i}\frac{1}{\beta_1 - K_{22}}\right|_{k_i = k_n} \tag{A9}$$

$$\frac{\partial\beta_i}{\partial k_i} = \left.\frac{\partial K_{11}}{\partial k_i}\right|_{k_i = k_n} \tag{A10}$$

Copyright © 2000 John Wiley & Sons, Ltd

in which

$$\left.\frac{\partial K_{11}}{\partial k_i}\right|_{k_i=k_n} = \frac{\partial}{\partial k_i}\left\{\frac{1}{N}\sum_{i=1}^{N}\frac{k_i}{k_n}\right\} = \frac{1}{Nk_n} \tag{A11}$$

$$\left.\frac{\partial K_{21}}{\partial k_i}\right|_{k_i=k_n} = \frac{\partial}{\partial k_i}\left\{-\frac{1}{Nr}\sum_{i=1}^{N}\frac{k_i}{k_n}y_i\right\} = -\frac{y_i}{rNk_n} \tag{A12}$$

Finally, $\phi_{11}=1$, $\phi_{21}=0$ and $\beta_1=1$ when evaluated at the nominal stiffness $k_i=k_n$. Substituting these into the expressions above yields Equations (21)–(28).

REFERENCES

1. *Uniform Building Code*. International Conference of Building Officials: Whittier, CA, 1997.
2. *NEHRP Recommended Provisions for Seismic Regulations for New Buildings*. Federal Emergency Management Agency (FEMA); 1997.
3. *Guide Specifications for Seismic Isolation Design*. American Association of State Highway and Transportation Officials: Washington, DC, 1991.
4. Shenton III HW. Guidelines for pre-qualification, prototype and quality control testing of seismic isolation systems. *NISTIR 5800,* National Institute of Standards and Technology, Gaithersburg, Maryland, 1996.
5. De La Llera JC, Chopra AK. Accidental torsion in buildings due to stiffness uncertainty. *Earthquake Engineering and Structural Dynamics* 1994; **23**(2): 117–136.
6. De La Llera JC, Chopra AK. Accidental torsion in buildings due to base rotation excitation. *Earthquake Engineering and Structural Dynamics* 1994; **23**(9): 1003–1021.
7. De La Llera JC, Chopra AK. Estimation of accidental torsion effects for seismic design of buildings. *Journal of Structural Engineering* 1995; **121**(1): 102–114.
8. Hirata K, Shiojiri H, Mazda T, Kontani O. Response variability of isolated structure due to randomness of isolation devices. *ICOSSAR '89, Proceedings of the 5th International Conference on Structural Safety and Reliability,* San Francisco, 7–11 August 1989.
9. De La Lera JC, Inaudi JA. Analysis of base-isolated buildings considering stiffness uncertainty in the isolation system. *Proceedings of the Fifth National Conference on Earthquake Engineering*, vol. I, 1994; 623–632.
10. Ang AH, Tang WH. *Probability Concepts in Engineering Planning and Design*, *vol. I*, *Basic Principles*. Wiley: New York, 1975.

Copyright © 2000 John Wiley & Sons, Ltd